Biomechanical behaviour of human bile duct wall and impact of cadaveric preservation processes.

Edouard Girard, Grégory Chagnon, Emeric Gremen, Maxime Calvez, Christopher Masri, Jean Boutonnat, Bertrand Trilling, Benjamin Nottelet

Biomechanical behaviour of human bile duct wall and impact of cadaveric preservation processes.

E. Girard[a,c,d,*] edouard.girard@univ-grenoble-alpes.fr, G. Chagnon[b], E. Gremen[d], M. Calvez[b], C. Masri[b], J. Boutonnat[e], B. Trilling[a,c,d], B. Nottelet[f]

[a]Univ. Grenoble Alpes, CNRS, Grenoble INP, CHU Grenoble Alpes, TIMC-IMAG, 38000, Grenoble, France

[b]Univ. Grenoble Alpes, CNRS, Grenoble INP, TIMC-IMAG, 38000, Grenoble, France

[c]Département de Chirurgie Digestive et de l'urgence, Centre Hospitalier Grenoble-Alpes, 38000, Grenoble, France

[d]Laboratoire d'anatomie des Alpes françaises (LADAF), UFR de Médecine de Grenoble, France

[e]Département d'anatomopathologie et Cytologie, Centre Hospitalier Grenoble-Alpes, 38000, Grenoble, France

[f]IBMM, Université de Montpellier, CNRS, ENSCM, Montpellier, France

*Corresponding author. Laboratoire TIMC-IMAG, Domaine de la Merci, 38706, La Tronche Cedex, France.

Abstract

Biliary diseases are the third most common cause of surgical digestive disease. There is a close relationship between the mechanical performance of the bile duct and its physiological function. Data of biomechanical properties of human main bile duct are scarce in literature. Furthermore, mechanical properties of soft tissues are affected by these preservation procedures. The aim of the present work was, on the one hand, to observe the microstructure of the human bile duct by means of histological analysis, on the other hand, to

characterize the mechanical behavior and describe the impact of different preservation processes. A mechanical study in a controlled environment consisting of cyclic tests was made. The results of the mechanical tests are discussed and explained using the micro-structural observations. The results show an influence of the loading direction, which is representative of an anisotropic behavior. A strong hysteresis due to the viscoelastic properties of soft tissues was also observed. Embalming and freezing preservation methods had an impact on the biomechanical properties of human main bile duct, with fiber network deterioration. That may further provide a useful quantitative baseline for anatomical and surgical training using embalming and freezing.

Keywords :Bile ducts; Mechanical phenomena; Anisotropy; Embalming; Freezing; Soft tissue

1 Introduction

In the field of biomedical engineering and surgical areas, the understanding of the mechanical macroscopic behavior of human soft tissues is primordial in order to design and develop novel treatment solutions. Nowadays, different in vivo characterization methods exist. Some have the benefit of being noninvasive, such as elastography which estimates the elasticity of the tissue (Ophir et al., 1991). Other techniques, like nano-indentation (Samur et al., 2007) or aspiration devices (Nava et al., 2004), are a bit more invasive. These methods, however, only allow for simple tests, unlike the classical ex vivo characterization which allows the observation of more complex behaviors, like large strain deformations or viscoelasticity.

Obviously, experimentation on in vivo human tissues is unthinkable for ethical grounds, and animal testing is increasingly difficult both in terms of logistics and ethics reasons. Use of anatomical pieces, i.e. post mortem humans tissues is an alternative to the above experimentations. However, the inconsistency and unpredictability of the donated bodies, as well as time between tissues sampling and mechanical experiments play against us. Not only is the experiment on fresh tissues difficult but the results are often not reproducible. Another difficulty when using fresh soft tissues for ex-vivo experimentations is that mechanical properties changes over time (Duch et al., 2002). Different preservation processes are commonly used in anatomical laboratory such as freezing and embalming, in order to avoid tissue degradation before experimentation (Cartner et al., 2011a; Coleman and Kogan, 1998). Mechanical properties of soft tissues are affected by these preservation procedures (Cartner et al., 2011a; Verstraete et al., 2015). There is no data on literature about characteristics and proportions of the mechanical modification induced by freezing or embalming on bile ducts tissues.

The bile duct system is divided into intrahepatic and extrahepatic bile ducts. Human extra-hepatic bile duct tract is responsible for transporting, storing and releasing bile into the digestive tract to aid digestion of fats (Al-Atabi et al., 2012). In terms of histological and morphological description, most of the biliary tract has already been investigated, i.e. the intra-hepatic bile ducts, the gallbladder (W. C. Li et al., 2013), the sphincter of Oddi and the cystic duct. The data concerning the extrahepatic main duct are scarce. The bile duct is lined by a single layer of columnar cells and its wall consists of intermixed dense fibrous tissue, elastic and collagen fibers in different proportion (Cha et al., 2007; Duch et al., 2002; Takahashi et al., 1985), and muscle fibers in low quantity (Hong et al., 2000; Walsh and Akoglu, n.d.).

Biliary diseases are the third most common cause of surgical digestive disease. There is a close relationship between the mechanical performance of the bile duct and its physiological function. Also, most pathologies, such as biliary lithiasis, cirrhotic liver, cholestasis and cholangitis, are treated using medical devices that interact with the bile duct. For example, biliary reconstruction during liver transplantation is a significance source of complications. We proved that internal biliary stent insertion during liver transplantation decreased postoperative morbidity (Girard et al., 2018). Biliary stent placement becomes common with the future development of degradable stents (Mauri et al., 2013; Tashiro et al., 2009). Therefore, knowledge of its bile duct mechanical behavior can improve the design of such devices.

The mechanical behavior of most tissues and organs has already been extensively studied (Abé et al., 1996), but data on extra-hepatic main biliary tract remains scarce. Several studies on the modeling of the human biliary system have been carried out. They mostly investigate bile rheology or bile fluids dynamics (Li et al., 2007; Luo et al., 2007). The focus is usually given to the properties of the gallbladder or cystic duct (Al-Atabi et al., 2012; W. G. Li et al., 2013; Luo et al., 2007). To the authors' knowledge, a single study by Li et al. (W. C. Li et al., 2013) provides data of biomechanical properties of the human main bile duct. They studied compliance of the cadaveric human bile duct by performing pressure tests. Apart from that, there are no experimental data available for the mechanical behavior of the human extra-hepatic main biliary duct wall at the present time. All the other available data were produced on animals, usually using canine or porcine models (Jian and Wang, 1991; Duch et al., 2002, 2004; W. C. Li et al., 2013). The similarities between the human and the porcine bile duct were studied (W. C. Li et al., 2013), and it was concluded that the pig's bile duct properties match that of the human.

The aims of this study were, on the one hand, to observe the microstructure of the human bile duct by means of histological analysis, on the other hand, to characterize the mechanical behavior and describe the impact of different preservation processes

using comparative experimental tensile tests. The results of the mechanical tests are discussed and explained using the micro-structural observations.

2 Materials and methods

2.1 Anatomical description of extrahepatic biliary tract

The biliary tract emerges from the liver and ends with the major duodenal papilla. In the liver, the bile canaliculi merge into the segmental bile ducts. The left and the right hepatic duct unite into the common hepatic duct. A common distinction is made between intra- and extra-hepatic bile ducts. Fig. 1 represents an anatomic specimen of extrahepatic biliary tract after dissection (a) with an illustration of the corresponding parts of extrahepatic bile ducts (b). The extrahepatic bile duct starts right under the hepatic hilum. The gallbladder is located under the liver. From its medial side arises the cystic duct, which merges with the common hepatic duct to become the common bile duct. Gallbladder and the cystic duct form the accessory bile duct. The main bile duct includes the common hepatic duct and the common bile duct.

Fig. 1

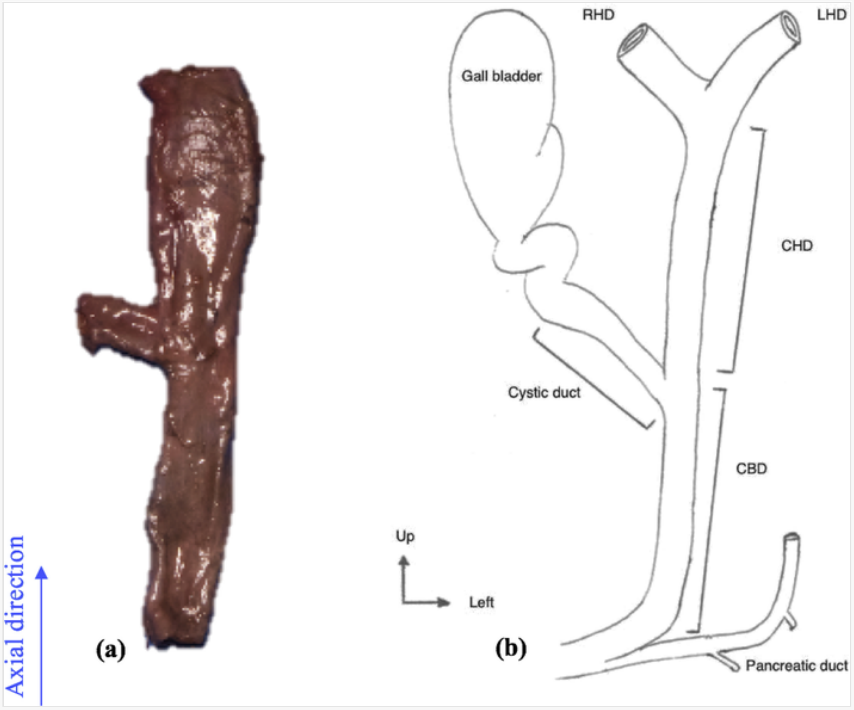

a. Anatomic specimen of extrahepatic biliary tract after dissection; b. Illustration of the corresponding parts of extrahepatic bile ducts.RHD: right hepatic duct; LHD: left hepatic duct; CHD: common hepatic duct; CBD: common bile duct.

2.2 Sample extraction and methodology

Cadavers were selected for anatomical dissection from the Anatomy laboratory, faculty of medicine, Grenoble, France (LADAF - Laboratoire d'Anatomie Des Alpes Françaises). This study was performed in compliance with French regulations on postmortem testing, and the protocol was approved by a local scientific committee of the Grenoble-Alpes University.

Even if it is preferable to only test fresh cadavers, it is often difficult to have ones, and the cadavers are mainly treated with a preservation process. In order to compare the different preservation process, three random groups were made, with frozen cadavers in the first group (G1), embalmed cadavers in the second group (G2) and fresh cadavers in the third group (G3). In G1, cadavers were immediately entirely frozen on arrival to the LADAF. Cadavers randomized in G2 were embalmed with a formalin solution (ARTHYL®) injected into the carotid artery and drained from the jugular vein (9 L with a formaldehyde concentration of 1.3%), and then preserved in a refrigerated room at 4°C. For G3, samples were collected on fresh cadavers immediately after their arrival in the LADAF. A maximum period of 48 h was tolerated between the date of death and the biomechanical tests. Preservation time is defined as the time between the beginning of the preservation process and the biomechanical tests.

The main peritoneal cavity was approached by a right subcostal incision. A section of the falciform ligament was realized if necessary. The hepatic pedicle was opened and its components separated. Then the biliary tract was severed in three spots: the cystic duct, the common bile duct upstream of the major duodenal papilla, and the hepatic duct downstream of intrahepatic bile ducts junction.

Cadavers defrosting was done according to our local protocol, established from previous experiments. Cadavers were placed in a 18°C temperate room. A percutaneous temperature sensor was set up in intraabdominal through the left flank. The defrosting process was considered complete when the intra-abdominal temperature reached 4 ° C.

Our study includes 12 anatomical dissections, without apparent hepato-biliary pathology, aged between 56 and 104 years (mean age 83±6 years). Nine of the extracted samples were used for mechanical testing; demographical statistics are represented in Table 1. Three samples were included in paraffin for histological observations.

alt-text: Table 1

Table 1

The presentation of Tables and the formatting of text in the online proof do not match the final output, though the data is the same. To preview the actual presentation, view the Proof.

Demographical statistics on cadavers used for mechanical experiments.

	Frozen *(G1)*	**Embalmed *(G2)***	**Fresh *(G3)***	***p***
Number of samples	3	3	3	
Sex ratio	1:2	2:1	1:2	0,67
Age *(years)*	88±14	88±8	76±20	0,32
BMI *($kg.m^{-2}$)*	20±2	18±1	19±2	0,33
Preservation time *(hours)*	84±62	90±27	-	0,88

Mean±standard deviation. BMI: Body Mass Index. Preservation time is that between the beginning of the preservation process and the mechanical tests. p: p-value, statistical significance if $p<0,05$.

2.3 Histology

Three common bile duct removed on fresh cadavers were chosen for histological analysis. Axial and circumferential sections of 1 cm on all samples were performed in the middle of the common bile duct. Samples were conserved in formaldehyde, fixed first in formalin 10% during 24 h at 4°C and then embedded in paraffin according to usual protocol (Canene-Adams, 2013). Sections of 3 μm were then realized with a microtome Leica RM 2245 (Wetzlar, Germany). The slides were then stained with Hematoxylin Eosin Saffron (HES) to see nucleic acids and connective tissue (amongst other collagen), or with Orscein staining to highlight elastin fibers. Sections were dewaxed, rehydrated, and the antigen retrieval was performed with a preheated protease. Antibody binding was detected using the ultraView Universal DAB Detection kit (Automate Benchmark XT IHC/ISH (ROCHE–VENTANA) 760–500) and 3,3-diaminobenzidine (DAB) as chromogen. Slides were then examined qualitatively by light microscopy focusing particularly on elastin and collagen fibers' orientation. Pictures were acquired by a digital camera (Leica Microsystems) connected to an optical microscope (Leica Microsystems).

2.4 Mechanical tests

Samples were tested as soon as possible after explantation, during which they were preserved in a saline solution. A maximum period of 48 h was tolerated between the date of death and the biomechanical tests. Tests were carried out by means of a GABO Eplexor 500N mechanical test machine with a 25N load cell. In order to respect physiological experimental conditions, an experimental thermo-regulated tank filled with 0.9% sodium chloride solution was designed. It was previously presented in Breche

et al. (2016) and already used for urethra (Masri et al., 2018). The saline solution was heated to a temperature of $37 \pm 1 \circ C$.

It was decided to perform planar tension test to obtain a greater tensile force compared to uniaxial extension and to reduce experimental noises and errors, and it was not possible to perform biaxial tests. The bile duct was cut and unraveled along its axial direction, as illustrated in Fig. 2a. Rectangular specimens of 48.2 ± 0.3 mm width, 0.5 ± 0.1 mm thickness and 10 mm height were gathered from the main bile duct along the axial direction, and 20.9 ± 0.4 mm width, 0.5 ± 0.1 mm thickness and 10 mm height for the circumferential direction, as shown in Fig. 2b. The samples were mounted in a rigid structure containing clamps outside the tank in order to ensure a consistent geometry for the samples, i.e., a fixed height of 2 mm and a width large enough (≥ 20 mm) so that the samples stay rectangular throughout the tests. Fig. 2c shows the rigid clamps-sample assembly which was then transferred into the testing apparatus. During the test, it is supposed that the sample stays rectangular and border effects are neglected (Charlton et al., 1994). The test is described by the deformation gradient tensor $\overline{\overline{F}}$. Non-porous soft tissues are classically considered incompressible (Holzapfel et al., 2004), which translates into $\det(\overline{\overline{F}}) = 1$. This implies that in planar tension condition $\overline{\overline{F}}$ can be written as:

$$\left[\overline{\overline{F}}\right] = \begin{bmatrix} \lambda & 0 & 0 \\ 0 & 1 & 0 \\ 0 & 0 & \frac{1}{\lambda} \end{bmatrix} \quad (1)$$

where $\lambda = \frac{l}{l_0}$ is the stretch (l and l_0 are the current and initial height of the specimen, as can be seen in Fig. 2c). It was decided to evaluate the influence of the preservation process on the initial behavior of the soft tissues, then simple tests with a few number of cycles were used. Each sample underwent a cyclic planar tension test consisting of a series of loading and unloading phases then a loading until rupture at a constant strain rate of $5.10^{-3}\,s^{-1}$ imposed by the testing machine. The strain rate was chosen sufficiently slow to avoid dynamic phenomena and to be closed to the clinical applications. For axial direction tests, 2 cycles at 5% strain followed by 2 cycles at 10% strain were performed. For circumferential direction tests, 2 cycles at 20% strain were performed. The number of specimens being limited, it was decided to perform tests different in the two directions. The objective is to perform loading cycles in the non-hardening zone of the material. The mechanical properties being very different in the two directions, the experimental protocol was also chosen different. The tests are analyzed by measuring the nominal stress defined as:

$$\Pi = \frac{F}{A_0} \quad (2)$$

where F is the force and A_0 the initial cross section.

Fig. 2

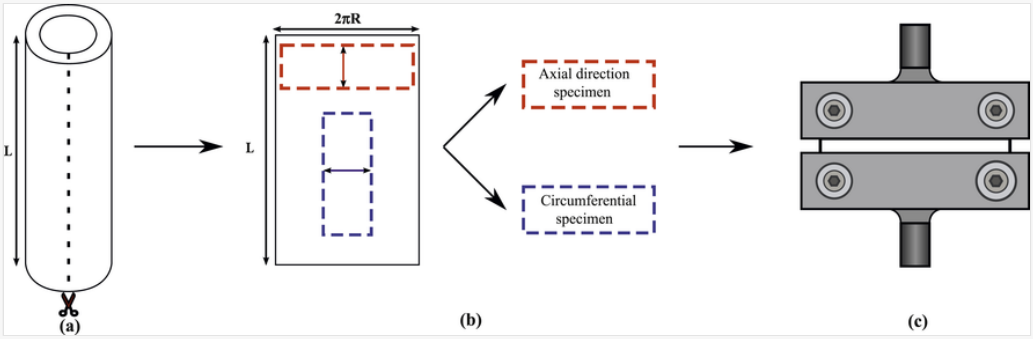

a. Bile duct cut along its axial direction. b. Planar tension specimens gathered from the unfolded bile duct. c. Specimen inserted in the clamps before transfer into the thermostatic tank.

2.5 Statistical analysis

Evidently, due to the nature of the present work based on post-mortem studies, the number of samples is limited for statistical analysis, but sufficient to ensure reproducibility. All data are presented as mean ± standard deviation. Continuous variables using the Mann–Whitney test or an ANOVA test for more than two modalities were compared, and categorical variables using the Fisher exact test. A difference was considered to be statistically significant at $p<0.05$.

3 Results

3.1 Histological analysis

Starting from the lumen to the outer diameter of the tissue in the circumferential plane, the bile duct is composed of four layers shown in Figs. 3–5: the mucous layer numbered 1, corresponding to a simple cylindrical epithelium measuring approximately 20 μm thickness. Beneath a lamina propria (chorion), corresponding to submucosal connective tissue divided into an internal submucosal layer, numbered 2, and an external submucosal layer, numbered 3, of 60-80 μm thickness each. Everything is surrounded by an adventitia, numbered 4, composed of loose conjunctive tissue containing vascular and nervous axes.

Fig. 3

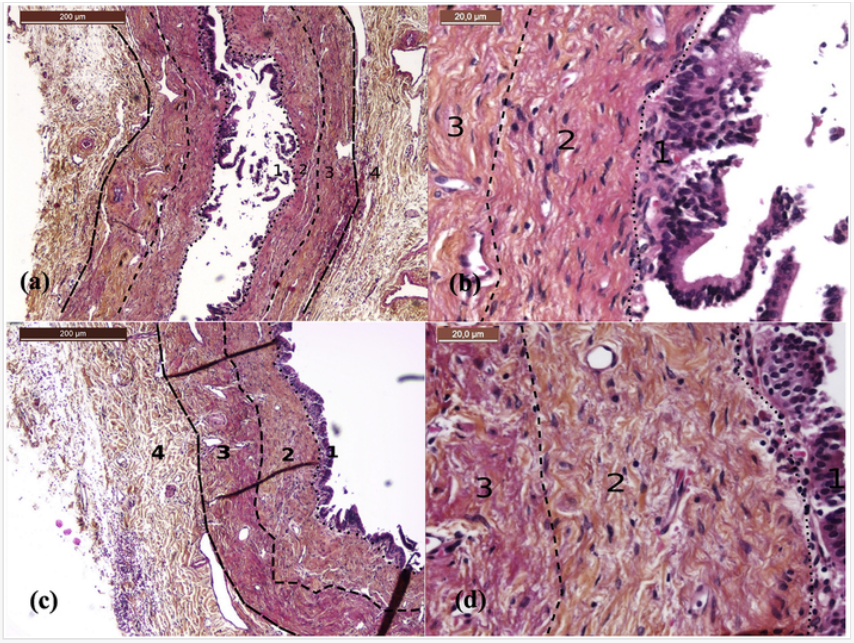

HES staining.a. axial section *x4*; b. axial section *x20*; c. circumferential section *x4*; d. circumferential section *x20*. Layers: epithelium (1), lamina propria with internal submucosa (2) and external submucosa (3) and adventitia (4).Cells were purple stained (dark purple for nucleus, light purple for cytoplasm). The collagen was orange stained, composed submucosal and adventitial layers without specific organization. Smooth muscle fibers were pink stained. They had a specific orientation with a different distribution in the submucosa layers. . (For interpretation of the references to colour in this figure legend, the reader is referred to the Web version of this article.)

Fig. 4

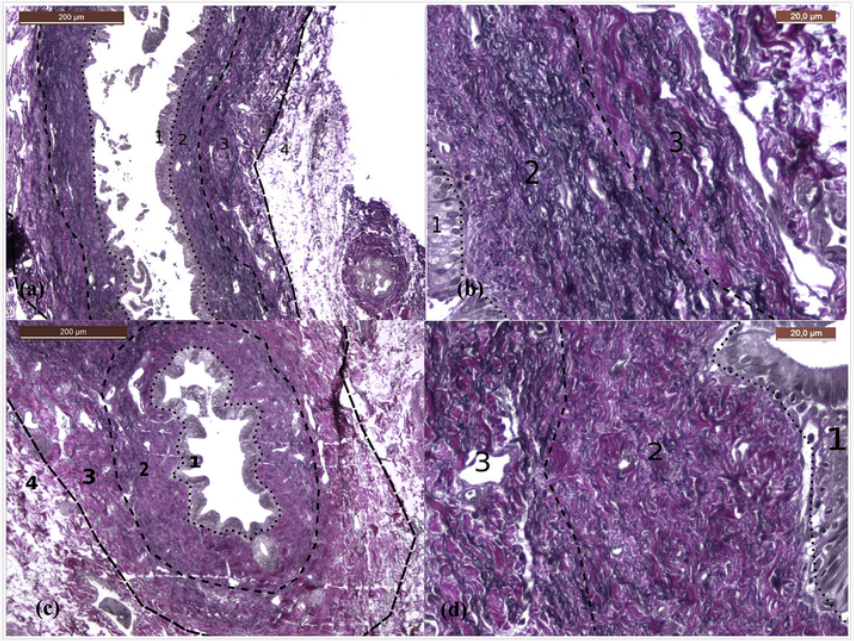

Orcein staining.a. axial section *x4*; b. axial section *x20*; c. circumferential section *x4*; d. circumferential section *x20*. Layers: epithelium (1), lamina propria with internal submucosa (2) and external submucosa (3) and adventitia (4).Elastic fibers were deep blue stained. Fibers were oriented

longitudinally in the internal layer and transversely in the external layer, with a greater proportion of longitudinal fibers. . (For interpretation of the references to colour in this figure legend, the reader is referred to the Web version of this article.)

Fig. 5

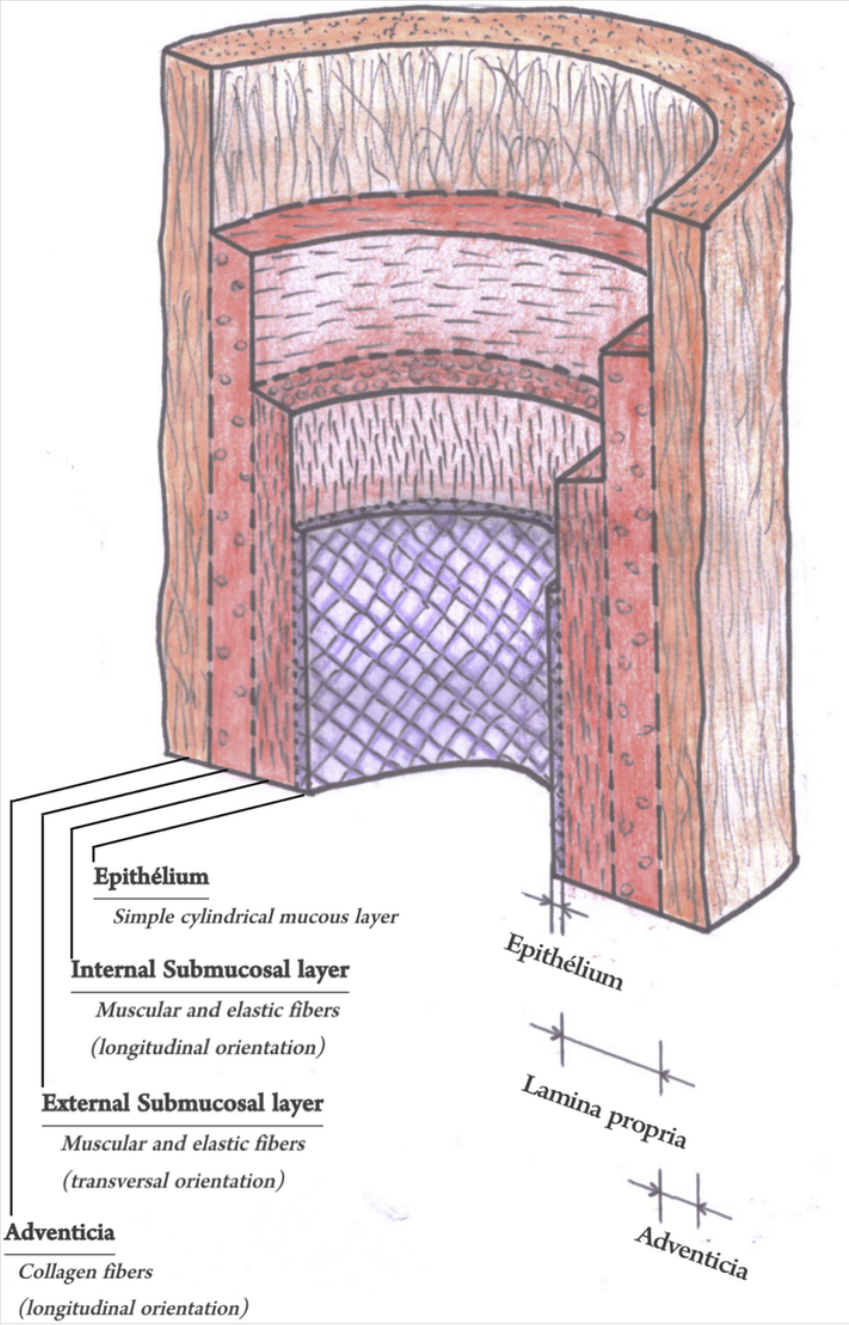

3D illustration of the main bile duct. Only the 4 main layers are represented along with the main fiber directions.

On HES staining (Fig. 3), cells were purple stained (dark purple for nucleus, light purple for cytoplasm). Bordering the lumen, the simple columnar epithelium was abraded. In the submucosal connective layer, the visualized cells correspond to fibroblasts or

lymphoid cells with a predominant distribution right under the basement membrane. Smooth muscle fibers were highlighted in pink using HES staining. They had a specific orientation with a different distribution in the submucosal layers. On the axial section (Fig. 3ab), they had a predominant distribution on the internal submucosa (layer 2), with longitudinal orientation. On the circumferential section (Fig. 3cd), fibers had a predominant distribution in the external submucosa (layer 3), with a transversal orientation. Concerning the conjunctive tissue, collagen fibers were orange stained on HES. They had a uniform distribution in the lamina propria layer without any specific orientation, regardless of the section. The adventitious layer contained very thick collagen fibers with a predominant longitudinal orientation.

The orcein staining enabled the visualization of the elastic fibers (deep blue) as illustrated in Fig. 4. These orcein stained sections confirmed the muscle fibers distribution in the submucosal layers. Fibers were oriented longitudinally in the internal layer and transversely in the external layer, with a greater proportion of longitudinal fibers. Geometrically, the angle of orientation of the fibers of the different layers in relation to the axis of the lumen was difficult to measure. However, the transverse and longitudinal elastic fibers appear to be orthogonal.

The histological observations are synthetized in the 3D illustration Fig. 5.

3.2 Mechanical behavior

3.2.1 Description of the experimental curves

Histological observations proved that specimens were cut in the symmetry axes of the materials, ensuring that the planar tensile test hypothesis was respected. Fig. 6 compared the results of planar tension tests in the three studied groups (G1: frozen group, G2: embalmed group, G3: fresh group), for both directions. Only one representative result is presented in each figure as the results on the different anatomical dissections were very close. By observing the first loads only, tissues present a nonlinear response to an applied strain with a strain hardening at large deformation, which is typical of a soft tissue. A hysteresis is observed, highlighting the viscoelastic behavior of the bile duct. Considering two successive loading cycles, a stress softening can be observed between the first and second loading. A vertical line is observed at the end of each loading curve, this is due to experimental machine that needs some seconds to change the direction of loading, and thus it is creating a relaxation of some seconds in the tests.

Fig. 6

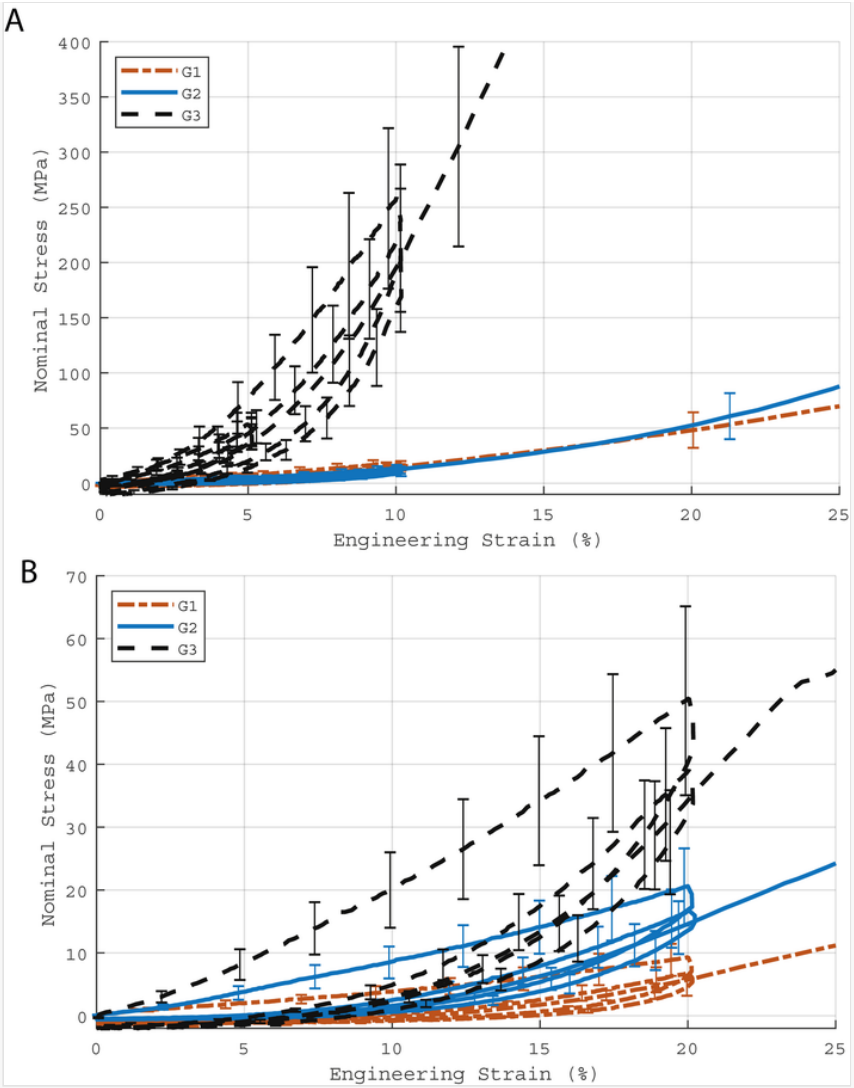

Experimental results of planar tension tests in the 3 studied groups for both directions. A: axial direction, B: circumferential direction.

Residual strain is also observed after each cycle, it is characterized by stress reaching zero while strain was still positive. This residual strain increases with the maximum strain applied to the material throughout the cycles.

No conclusions could be deduced on the possibility to recover this residual strain due to the limited number of specimens and to the limited time of the test. To measure if this residual strain in permanent or not, very long relaxation time should be imposed but they can lead also to the deterioration of the specimens. After removing the samples from the testing machine, no return of the specimens to their initial configuration was observed even after a long waiting time suggesting an irreversible effect to this residual strain.

It is important to note that the value of the stress lower than 0 should not be trusted as the specimen was compressed and local buckling occurred. Whatever the group, the

bile duct presents an anisotropy, i.e. stiffer mechanical behavior in the axial direction compared to the circumferential one. As a comparison, for example for a strain of 10%, the nominal stress in the axial direction is 250 MPa where it is 20 MPa in the circumferential one for the G3 group meaning that the difference of mechanical behavior is very important according to the direction. The same phenomenon is observed for the G1 and G2 groups but to a lesser extent.

3.2.2 Comparison of the three groups

Different quantities were measured and calculated according to the curves of Fig. 6 in order to compare easily the different groups. The slope of the curves (engineering stress - engineering strain) were evaluated, corresponding to the local tangent stiffness of the engineering strain-stress curve of the tissue. They were calculated during the loading and unloading phases on a 2 or 4 percent strain interval. All these slopes were evaluated for the three groups (G1, G2 and G3) and for the two directions (circumferential and axial), they are summarized in the Tables 2 and 3 and illustrated in Figs. 7 and 8. These slopes have no physical meaning but are local synthetic values that permits to compare the different tests.

alt-text: Table 2

Table 2

The presentation of Tables and the formatting of text in the online proof do not match the final output, though the data is the same. To preview the actual presentation, view the Proof.

Slope of the curves and hysteresis for 3 comparative groups experimental planar tension tests in axial direction.

Axial	1st load		1st unload		Loading energy	Hysteresis energy	Ratio of hysteresis
	0-2%	2-4%	0-2%	2-4%			
G1	6,03	5,86	2,27	5,26	0,60	0,20	33%
(Frozen)	(2,79)	(3,75)	(1,02)	(2,77)	(0,35)	(0,08)	
G2	5,69	6,21	2,86	5,59	0,45	0,12	27%
(Embalmed)	(2,33)	(4,00)	(2,07)	(3,29)	(0,25)	(0,06)	
G3	**19,50**	**37,46**	**8,91**	**28,58**	**1,28**	**0,49**	**38%**
(Fresh)	(14,78)	(37,04)	(6,57)	(28,18)	(0,68)	(0,25)	
p	*0,17*	*0,20*	*0,16*	*0,22*			
Axial	2nd load		2nd unload		Loading	Hysteresis	Ratio of

	0-2%	2-4%	0-2%	2-4%	energy	energy	hysteresis
G1	4,33	6,79	4,33	6,79	0,49	0,11	22%
(Frozen)	(1,68)	(3,61)	(1,68)	(3,61)	(0,24)	(0,07)	
G2	**4,54**	**6,76**	**4,54**	**6,76**	**0,40**	**0,09**	**21%**
(Embalmed)	(2,80)	(3,62)	(2,80)	(3,62)	(0,17)	(0,03)	
G3	**16,31**	**37,17**	**16,31**	**37,17**	**1,42**	**0,54**	**38%**
(Fresh)	(13,16)	(36,47)	(13,16)	(36,47)	(0,92)	(0,28)	
p	*0,18*	*0,21*	*0,20*	*0,21*			

Axial	3rd load	3rd unload	4th load	Hysteresis
	8-10%	8-10%	8-10%	
G1	11,26	15,88	12,97	121,91
(Frozen)	(10,45)	(12,47)	(10,81)	(52,20)
G2	**11,39**	**15,73**	**14,08**	**129,51**
(Embalmed)	(6,50)	(7,94)	(7,38)	(69,90)
G3	**132,72**	**160,29**	**151,87**	**846,47**
(Fresh)	(170,47)	(199,24)	(196,88)	(977,16)
p	*0,29*	*0,28*	*0,30*	*0,27*

Mean (standard deviation) *(kPa), p: p-value, statistical significance if p<0,05.*

alt-text: Table 3

Table 3

The presentation of Tables and the formatting of text in the online proof do not match the final output, though the data is the same. To preview the actual presentation, view the Proof.

Slope of the curves and hysteresis for 3 comparative groups experimental planar tension tests in circumferential direction.

circumferential	**1st load**			**1st unload**			**Loading energy**	**Hysteresis energy**	**Ratio of hysteres**
	0-4%	**4-8%**	**16-20%**	**0-4%**	**4-8%**	**16-20%**			
G1	1,27	1,33	1,89	0,21	0,40	3,77	1,72	0,82	47%
(Frozen)	(1,08)	(1,18)	(1,51)	(0,24)	(0,45)	(3,10)	(1,42)	(0,53)	

G2	**1,90**	**2,74**	**3,91**	**0,20**	**0,59**	**7,00**	**2,20**	**1,18**	**54%**
(Embalmed)	(2,69)	(3,79)	(4,96)	(0,14)	(0,62)	(9,47)	(1,61)	(0,84)	
G3	**3,21**	**4,27**	**6,57**	**0,26**	**0,77**	**11,87**	**5,81**	**2,90**	**50%**
(Fresh)	(3,02)	(4,65)	(5,68)	(0,28)	(0,99)	(10,87)	(4,01)	(1,71)	
p	*0,63*	*0,62*	*0,48*	*0,93*	*0,82*	*0,54*			

circumferential	2nd load			2nd unload			Loading energy	Hysteresis energy	Ratio of hysteresis	Hy
	0-4%	4-8%	16-20%	0-4%	4-8%	16-20%				
G1	0,36	0,62	2,75	0,19	0,32	3,59	1,03	0,27	26%	74
(Frozen)	(0,35)	(0,61)	(2,24)	(0,21)	(0,36)	(2,87)	(0,74)	(0,17)		(58
G2	**0,38**	**1,00**	**5,31**	**0,16**	**0,45**	**6,83**	**1,17**	**0,43**	**36%**	**12**
(Embalmed)	(0,28)	(1,23)	(6,69)	(0,06)	(0,43)	(8,88)	(0,82)	(0,24)		(16
G3	**0,50**	**1,35**	**9,15**	**0,28**	**0,56**	**11,31**	**3,20**	**0,94**	**29%**	**19**
(Fresh)	(0,53)	(1,59)	(8,05)	(0,15)	(0,03)	(6,01)	(2,41)	(0,61)		(17
p	*0,91*	*0,77*	*0,47*	*0,65*	*0,86*	*0,51*				*0,5*

Mean (standard deviation) *(kPa), p: p-value, statistical significance if p<0,05.*

Fig. 7

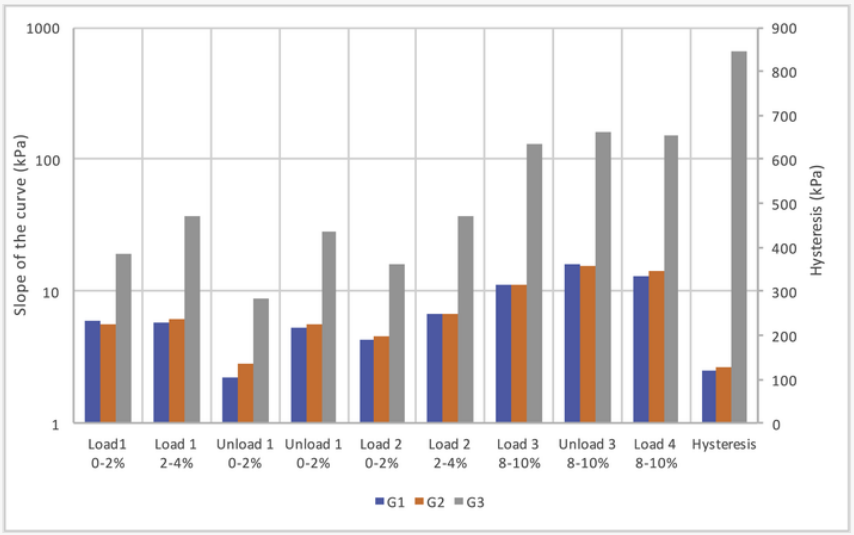

Slopes of the curves representation for 3 comparative groups experimental planar tension tests in axial direction.

Fig. 8

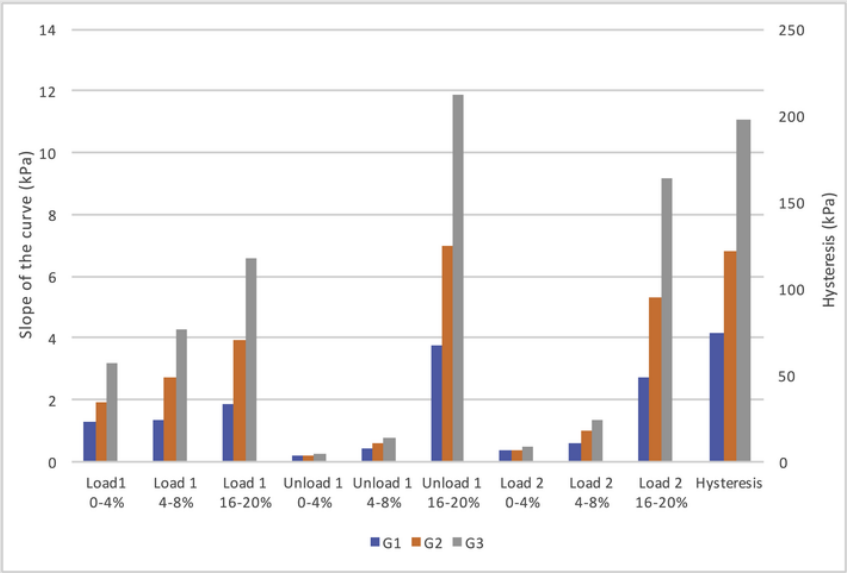

Slopes of the curves representation for 3 comparative groups experimental planar tension tests in circumferential direction.

The observations are different according to the direction of the loading. In the axial direction, it appears that the values are very close for the G1 and G2 groups but are far from the G3 group, the values are different from a factor 3 to 10. In the circumferential direction, the G1 and G2 groups are different and far from the G3 group, the ratio is not so important as in the axial direction. This illustrates that the properties are strongly affected by the preservation conditions, the slopes of every curves are strongly reduced.

To compare the energy dissipated during the cyclic process, the areas under the loading curves and the areas of the hysteresis loops in the engineering strain – engineering stress curves are evaluated for each test and each group. The values are summarized in the Tables 2 and 3 and illustrated in Figs. 7 and 8. The part of hysteresis is larger in the axial direction than in the circumferential one. It is to note that the amount of the elastic and hysteresis energy are largely influenced by the preservation conditions for the groups G1 and G2 but the ratio of the dissipated energy compared to the elastic one is nearly conserved.

4 Discussion

As mentioned earlier, only few studies have analyzed the mechanical behavior of the human bile duct. The objectives of this work were therefore to characterize the mechanical behavior of the human bile duct and to test different preservation conditions.

At first, a histological study was made in order to observe structure and orientation of the different components involved in the main bile duct. Histological observations allowed the interpretation of the mechanical tests. Globally, 3 types of fibers are to be differentiated because of their different mechanical properties, elastic fibers, muscular fibers and collagen fibers. The collagen fibers have a distribution in the lamina propria layer without specific orientation, but with an increasing density gradient from the external to the internal layer. Variously, the adventitia is exclusively composed of collagen fibers, mainly longitudinally oriented. Muscle fibers are present only in the lamina propria layer with a different orientation according to the sub-layers. They were oriented longitudinally in the internal sub-layer and transversally in the external layer with a greater fibers density in the internal sub-layer. As muscle fibers, elastic fibers are present only in the lamina propria layer, with the same orientations, but with a different distribution according to the sub-layers. There is a greater proportion of longitudinal elastic fibers in the internal submucosal layer compared to the external submucosal layer.

The anisotropic behavior of the main bile duct can be correlated with histological observations. The stiffer mechanical behavior in the axial direction compared to the circumferential one corresponds to the longitudinal orientation of the collagen fibers in the adventitious layer. Collagen provides tissues with tensile strength to resist deformation (Muiznieks and Keeley, 2013). Conversely, elastic fibers provide tissues with elasticity to withstand repetitive stress (Muiznieks and Keeley, 2013). The general behavior of the main bile duct in both directions can be explained by its physiological functions. The main bile duct stores the bile that is secreted continuously by the liver, to expel it only a few times a day during meals. During this storage period, the main bile duct endures large radial distension, with an increased pressure, which can explain its softer behavior in this direction (Kong, 2008; W. C. Li et al., 2013). This anisotropic behavior confirms the results of Li et al. obtained by performing pressure tests (W. C. Li et al., 2013).

The different preservation conditions of the biliary duct were investigated. The objective was to compare the values obtained after freezing or embalming in comparison to fresh specimens. The conclusions are summarized in Table 4. The use of a preservation process, even if it allows maintaining the shape of the organs, has important effects on the fiber structure of the biliary duct. Preservation processes do not modify the shape of the mechanical response; however, they do not faithfully reflect biomechanical characteristics of fresh specimens. In this case, the mechanical properties decrease almost by 80% in the axial direction and by 40 to 60% in the radial direction. The influence is more important in the axial direction because the collagen fibers, mainly present in the longitudinal orientation, are more impacted. In the same way, the preservation processes modify the hysteresis differences that are mainly greater for fresh tissues in the axial direction.

alt-text: Table 4

Table 4

The presentation of Tables and the formatting of text in the online proof do not match the final output, though the data is the same. To preview the actual presentation, view the Proof.

Relative variation of slopes of the curves and hysteresis means, for G1/G3 and G2/G3, in both directions.

		Slope of the curves		Hysteresis
		Relative variation means	Relative variation Standard deviations	
Relative variation	*Direction test*	*%*	*%*	%
G1/G3	Axial	82,0	8,3	85,6
	circumferential	54,2	19,1	62,4
G2/G3	Axial	81,0	9,0	84,7
	circumferential	33,2	8,2	38,8

Even if the two processes of preservation are different, they both affect the fiber network. The mechanical effects of embalming on connective tissues are complex, since, on one hand, the tissues are likely softened by partial denaturing of the collagen, while on the other hand, there are also effects of collagen cross-linking due to the formalin embalming solution (Fessel et al., 2011). The effects of collagen denaturing probably predominates over those of the formalin cross-linking. Muscle fibers modifications were also observed after embalming (Benkhadra et al., 2011). A fragmentation of the muscle proteins, probably caused by the embalming solution, could explain the suppleness of the bile duct. Biomechanical studies on different tissues after embalming confirm our observations, showing reduced mechanical performance of bone (Stefan et al., 2010) or tendons (Fessel et al., 2011) and a loss of 80 to 96% of the mechanical properties for the spine (Wilke et al., 1996).

For preservation by freezing, the reasons are different but the mechanical properties modifications are also present. Regarding microstructural modifications, the mean diameter of collagen fibrils and the fibril non-occupation mean ratio are increased, while the mean number of fibrils decreased (Giannini et al., 2008). Mechanical changes related to freezing appear to affect different organs; tendons and bones in the first place (Cartner et al., 2011a; Giannini et al., 2008).

The results in the literature are nevertheless discordant, with several studies that demonstrate a stiffening related to embalming (Bourgouin et al., 2012; Nazarian et al., 2009; Verstraete et al., 2015), and identical properties between fresh and frozen specimens tests (Clavert et al., 2001; Moon et al., 2006). The problem is that studies are not standardized, making comparison difficult. The results may change depending on many factors: the type of tested tissues, the embalming protocol, the freezing or defrosting protocols, the experimental conditions, the delay before experimentation, etc. The different studied tissues also respond differently to the embalmment process, because the formalin solution penetration is different according to the tissues. When a cadaver is arterially perfused, highly vascular skeletal muscle will be more readily penetrated than less vascular bone, tendon or bile duct. The standardization of embalmed protocol could avoid inter studies variations. Indeed, the injected formalin quantity, the formalin concentration or the injection technique could modify the properties. Colman et al. recommended a minimal formalin concentration between 0.5 and 0.75% (Coleman and Kogan, 1998). It was respected in this study, with an injection of 9L of solution for 500 ml of formaldehyde (25%) at a final concentration of 1.3%. This means that only half of the total volume could be used in others studies (Hayashi et al., 2014), knowing that a too high concentration can also damage the tissues.

The defrosting protocol was also important. For example, Cartner and al (Cartner et al., 2011b). demonstrated that the physical properties of bone may be detrimentally affected in biomechanical testing that exceeds the 50-h time point after removal from the freezer. However, to our knowledge, there is no standardized protocol in the literature. For the future, it will be interesting to assess the impact of defrosting on the mechanical behavior of the tissues. Mechanical properties depend on hydration state, with stiffening with drying (Verstraete et al., 2015). In our study, all the tissues were preserved from dehydration by plunging them as fast as possible into a physiologic solution. Experimentation were also realized in physiologic conditions, in a thermostatic tank.

The present study has several limitations. First, only samples from elder people have been analyzed. It is known that biological tissues loose water and collagen with age (Trabelsi et al., 2010), and therefore, their mechanical properties can be affected, so, a wider experimental test with higher range of ages should be performed to drive non-age dependent conclusions. Secondly, the biliary tissues are in contact with the bile, which is responsible for a postmortem deterioration of the surrounding tissues. The mechanical properties of the biliary tract changes over time with tissue deterioration (Duch et al., 2002). Even though we have minimized the delay between death and testing, the fact that they are not similar between the three groups induces a bias. Thirdly, the delay between death and the cadaver arrival in the laboratory is a limit that cannot be avoided because of the current legislation. To avoid this bias from influencing our study, cadavers must be treated less than 48 h after death. Finally, there is a

variability in the different experimental data that is related to the fact that all individuals are different. Therefore, more samples would be necessary to draw more accurate conclusions.

5 Conclusion

This study investigated the mechanical behavior of the main bile duct and compared the impact of different preservation processes. After a histomorphological analysis of the tissue, a mechanical study in a controlled environment consisting of cyclic tests was performed. The results show an influence of the loading direction, which is representative of an anisotropic behavior. A strong hysteresis due to the viscoelastic properties of soft tissues was also observed. This study confirmed that embalming and freezing preservation methods have an impact on the biomechanical properties of the human main bile duct. That may further provide a useful quantitative baseline for subsequent biomechanical studies or for anatomical and surgical training using embalming and freezing. Our work may improve our understanding of the mechanical properties of the main bile duct and will allow us in a further study to reproduce the bile duct behavior in computational models. That will help the digestive surgeons to detect anomalies and, when necessary, to choose the appropriate type of prosthesis in function of the specific patient.

Compliance with ethical standards

- Compliance with French postmortem testing regulations.
- Conflict of Interest: The authors declare that they have no conflict of interest.

Declarations of interest

None.

Acknowledgments:

P. Masson for dissections, P. Chaffanjon for postmortem regulations, M. Dalecky and B. Hodaj for histological analysis.

References

Abé, H., Hayashi, K., Sato, M. (Eds.), 1996. Data Book on Mechanical Properties of Living Cells, Tissues, and Organs, Springer Japan, Tokyo. Available from: https://doi.

org/10.1007/978-4-431-65862-7.

Al-Atabi, M., Ooi, R.C., Luo, X.Y., Chin, S.B., Bird, N.C., 2012. Computational analysis of the flow of bile in human cystic duct. Med. Eng. Phys. 34, 1177–1183. Available from: https://doi.org/10.1016/j.medengphy.2011.12.006.

Benkhadra, M., Bouchot, A., Gérard, J., Genelot, D., Trouilloud, P., Martin, L., Girard, C., Danino, A., Anderhuber, F., Feigl, G., 2011. Flexibility of Thiel's embalmed cadavers: the explanation is probably in the muscles. Surg. Radiol. Anat. 33, 365–368. Available from: https://doi.org/10.1007/s00276-010-0703-8.

Bourgouin, S., Bège, T., Masson, C., Arnoux, P.-J., Mancini, J., Garcia, S., Brunet, C., Berdah, S.V., 2012. Biomechanical characterisation of fresh and cadaverous human small intestine: applications for abdominal trauma. Med. Biol. Eng. Comput. 50, 1279–1288. Available from: https://doi.org/10.1007/s11517-012-0964-y.

Breche, Q., Chagnon, G., Machado, G., Girard, E., Nottelet, B., Garric, X., Favier, D., 2016. Mechanical behaviour′s evolution of a PLA-b-PEG-b-PLA triblock copolymer during hydrolytic degradation. J. Mech. Behav. Biomed. Mater. 60, 288–300. Available from: https://doi.org/10.1016/j.jmbbm.2016.02.015.

Canene-Adams, K., 2013. Preparation of formalin-fixed paraffin-embedded tissue for immunohistochemistry. Methods in Enzymology, Elsevier, pp. 225–233. Available from: https://doi.org/10.1016/B978-0-12-420067-8.00015-5.

Cartner, J.L., Hartsell, Z.M., Ricci, W.M., Tornetta, P., III, 2011. Can we trust ex vivo mechanical testing of fresh–frozen cadaveric specimens? The effect of postfreezing delays. J. Orthop. Trauma 25, 459–461.

Cartner, J.L., Hartsell, Z.M., Ricci, W.M., Tornetta, P., 2011. Can we trust ex vivo mechanical testing of fresh--frozen cadaveric specimens? The effect of postfreezing delays. J. Orthop. Trauma 25, 459–461. Available from: https://doi.org/10.1097/BOT.0b013e318225b875.

Cha, J.M., Kim, M.-H., Jang, S.J., 2007. Early bile duct cancer. World J. Gastroenterol. WJG 13, 3409.

Charlton, D.J., Yang, J., Teh, K.K., 1994. A review of methods to characterize rubber elastic behavior for use in finite element analysis. Rubber Chem. Technol. 67, 481–503. Available from: https://doi.org/10.5254/1.3538686.

Clavert, P., Kempf, J.F., Bonnomet, F., Boutemy, P., Marcelin, L., Kahn, J.L., 2001. Effects of freezing/thawing on the biomechanical properties of human tendons. Surg. Radiol. Anat. SRA 23, 259–262.

Coleman, R., Kogan, I., 1998. An improved low-formaldehyde embalming fluid to preserve cadavers for anatomy teaching. J. Anat. 192, 443–446. Available from: https://doi.org/10.1046/j.1469-7580.1998.19230443.x.

Duch, B.U., Andersen, H., Gregersen, H., 2004. Mechanical properties of the porcine bile duct wall. Biomed. Eng. Online 3, 23.

Duch, B.U., Andersen, H.L., Smith, J., Kassab, G.S., Gregersen, H., 2002. Structural and mechanical remodelling of the common bile duct after obstruction. Neuro Gastroenterol. Motil. 14, 111–122. Available from: https://doi.org/10.1046/j.1365-2982.2002.00310.x.

Fessel, G., Frey, K., Schweizer, A., Calcagni, M., Ullrich, O., Snedeker, J.G., 2011. Suitability of Thiel embalmed tendons for biomechanical investigation. Ann. Anat. - Anat. Anz. 193, 237–241. Available from: https://doi.org/10.1016/j.aanat.2011.03.007.

Giannini, S., Buda, R., Di Caprio, F., Agati, P., Bigi, A., De Pasquale, V., Ruggeri, A., 2008. Effects of freezing on the biomechanical and structural properties of human posterior tibial tendons. Int. Orthop. 32, 145–151. Available from: https://doi.org/10.1007/s00264-006-0297-2.

Girard, E., Risse, O., Abba, J., Medici, M., Leroy, V., Chirica, M., Letoublon, C., 2018. Internal biliary stenting in liver transplantation. Langenbeck's Arch. Surg.. Available from: https://doi.org/10.1007/s00423-018-1669-y.

S. Hayashi, H. Homma, M. Naito, J. Oda, T. Nishiyama, A. Kawamoto, S. Kawata, N. Sato, T. Fukuhara, H. Taguchi, K. Mashiko, T. Azuhata, M. Ito, K. Kawai, T. Suzuki, Y. Nishizawa, J. Araki, N. Matsuno, T. Shirai, N. Qu, N. Hatayama, S. Hirai, H. Fukui, K. Ohseto, T. Yukioka, M. Itoh. Saturated salt solution method: a useful cadaver embalming for surgical skills training. Medicine (Baltimore) 93 https://doi.org/10.1097/MD.0000000000000196, 2014.

Holzapfel, G.A., Gasser, T.C., Ogden, R.W., 2004. A new constitutive framework for arterial wall mechanics and a comparative study of material models. In: Cowin, S.C., Humphrey, J.D. (Eds.), Cardiovascular Soft Tissue Mechanics, Kluwer Academic Publishers, Dordrecht, pp. 1–48. Available from: https://doi.org/10.1007/0-306-48389-0_1.

Hong, S.-M., Kang, G.H., Lee, H.Y., Ro, J.Y., 2000. Smooth muscle distribution in the extrahepatic bile duct: histologic and immunohistochemical studies of 122 cases. Am. J. Surg. Pathol. 24, 660–667. Available from: https://doi.org/10.1097/00000478-200005000-00004.

Jian, C., Wang, G., 1991. Biomechanical study of the bile duct system outside the liver. Bio Med. Mater. Eng. 1, 105–113.

Kong, J., 2008. Choledochoscope manometry about different drugs on the Sphincter of Oddi. World J. Gastroenterol. 14, 5907. Available from: https://doi.org/10.3748/wjg.14.5907.

Li, W.C., Zhang, H.M., Li, J., Dong, R.K., Yao, B.C., He, X.J., Wang, H.Q., Song, J., 2013. Comparison of biomechanical properties of bile duct between pigs and humans for liver xenotransplant. Transplant. Proc. 45, 741–747. Available from: https://doi.org/10.1016/j.transproceed.2012.11.006.

Li, W.G., Hill, N.A., Ogden, R.W., Smythe, A., Majeed, A.W., Bird, N., Luo, X.Y., 2013. Anisotropic behaviour of human gallbladder walls. J. Mech. Behav. Biomed. Mater. 20, 363–375. Available from: https://doi.org/10.1016/j.jmbbm.2013.02.015.

Li, W.G., Luo, X.Y., Johnson, A.G., Hill, N.A., Bird, N., Chin, S.B., 2007. One-dimensional models of the human biliary system. J. Biomech. Eng. 129, 164–173. Available from: https://doi.org/10.1115/1.2472379.

Luo, X., Li, W., Bird, N., Chin, S.B., Hill, N.A., Johnson, A.G., 2007. On the mechanical behavior of the human biliary system. World J. Gastroenterol. WJG 13, 1384–1392.

Masri, C., Chagnon, G., Favier, D., Sartelet, H., Girard, E., 2018. Experimental characterization and constitutive modeling of the biomechanical behavior of male human urethral tissues validated by histological observations. Biomechanics Model. Mechanobiol.. Available from: https://doi.org/10.1007/s10237-018-1003-1.

Mauri, G., Michelozzi, C., Melchiorre, F., Poretti, D., Tramarin, M., Pedicini, V., Solbiati, L., Cornalba, G., Sconfienza, L.M., 2013. Biodegradable biliary stent implantation in the treatment of benign bilioplastic-refractory biliary strictures: preliminary experience. Eur. Radiol. 23, 3304–3310. Available from: https://doi.org/10.1007/s00330-013-2947-2.

Moon, D.K., Woo, S.L.-Y., Takakura, Y., Gabriel, M.T., Abramowitch, S.D., 2006. The effects of refreezing on the viscoelastic and tensile properties of ligaments. J. Biomech. 39, 1153–1157. Available from: https://doi.org/10.1016/j.jbiomech.2005.02.012.

Muiznieks, L.D., Keeley, F.W., 2013. Molecular assembly and mechanical properties of the extracellular matrix: a fibrous protein perspective. Biochim. Biophys. Acta BBA - Mol. Basis Dis. 1832, 866–875. Available from: https://doi.org/10.1016/j.bbadis.2012.11.022.

Nava, A., Mazza, E., Kleinermann, F., Avis, N., McClure, J., Bajka, M., 2004. Evaluation of themechanical properties of human liver and kidney through aspiration experiments. Technol. Health Care 12, 269–280.

Nazarian, A., Hermannsson, B.J., Muller, J., Zurakowski, D., Snyder, B.D., 2009. Effects of tissue preservation on murine bone mechanical properties. J. Biomech. 42, 82–86. Available from: https://doi.org/10.1016/j.jbiomech.2008.09.037.

Ophir, J., Céspedes, I., Ponnekanti, H., Yazdi, Y., Li, X., 1991. Elastography: a quantitative method for imaging the elasticity of biological tissues. Ultrason. Imag. 13, 111–134. Available from: https://doi.org/10.1177/016173469101300201.

Samur, E., Sedef, M., Basdogan, C., Avtan, L., Duzgun, O., 2007. A robotic indenter for minimally invasive measurement and characterization of soft tissue response. Med. Image Anal. 11, 361–373. Available from: https://doi.org/10.1016/j.media.2007.04.001.

Stefan, U., Michael, B., Werner, S., 2010. Effects of three different preservation methods on the mechanical properties of human and bovine cortical bone. Bone 47, 1048–1053. Available from: https://doi.org/10.1016/j.bone.2010.08.012.

Takahashi, Y., Takahashi, T., Takahashi, W., Sato, T., 1985. Morphometrical evaluation of extrahepatic bile ducts in reference to their structural changes with aging. Tohoku J. Exp. Med. 147, 301–309.

Tashiro, H., Ogawa, T., Itamoto, T., Ushitora, Y., Tanimoto, Y., Oshita, A., Amano, H., Asahara, T., 2009. Synthetic bioabsorbable stent material for duct-to-duct biliary reconstruction. J. Surg. Res. 151, 85–88. Available from: https://doi.org/10.1016/j.jss.2008.02.056.

Trabelsi, O., del Palomar, A.P., López-villalobos, J.L., Ginel, A., Doblaré, M., 2010. Experimental characterization and constitutive modeling of the mechanical behavior of the human trachea. Med. Eng. Phys. 32, 76–82. Available from: https://doi.org/10.1016/j.medengphy.2009.10.010.

Verstraete, M.A., Van Der Straeten, C., De Lepeleere, B., Opsomer, G.-J., Van Hoof, T., Victor, J., 2015. Impact of drying and thiel embalming on mechanical properties of achilles tendons: embalming and Drying of Tendons. Clin. Anat. 28, 994–1001. Available from: https://doi.org/10.1002/ca.22624.

Walsh, T.H., Akoglu, T., n.d. The Muscle Content and Contractile Capability of the Common Bile Duct 4.

Wilke, H.J., Krischak, S., Claes, L.E., 1996. Formalin fixation strongly influences biomechanical properties of the spine. J. Biomech. 29, 1629–1631.